Forced desorption of polymers from interfaces

2011 New J. Phys. 13 013025

(http://iopscience.iop.org/1367-2630/13/1/013025)

New Journal of Physics
The open-access journal for physics

Forced desorption of polymers from interfaces

Douglas B Staple[1,2], Michael Geisler[3], Thorsten Hugel[3], Laurent Kreplak[2] and Hans Jürgen Kreuzer[2,4]

[1] Max Planck Institut für Physik komplexer Systeme, Nöthnitzer Strasse 38, 01187 Dresden, Germany
[2] Department of Physics and Atmospheric Science, Dalhousie University, Halifax, NS, Canada
[3] Physics Department, IMETUM, CeNS Technische Universität München, Garching, Germany
E-mail: dstaple@pks.mpg.de, geisler@imetum.tum.de, hugel@imetum.tum.de, kreplak@dal.ca and h.j.kreuzer@dal.ca

New Journal of Physics **13** (2011) 013025 (20pp)
Received 30 August 2010
Published 19 January 2011
Online at http://www.njp.org/
doi:10.1088/1367-2630/13/1/013025

Abstract. In the past decade it has become possible to directly measure the adsorption force of a polymer in contact with a solid surface using single-molecule force spectroscopy. A plateau force in the force–extension curve is often observed in systems of physisorbed or noncovalently bonded polymers. If a molecule is pulled quickly compared to internal relaxation, then nonequilibrium effects can be observed. Here we investigate these effects using statistical mechanical models and experiments with a spider silk polypeptide. We present evidence that most experiments showing plateau forces are done out of equilibrium. We find that the dominant nonequilibrium effect is that the detachment height $h_{\max}(v)$ increases with pulling speed v. Based on a nonequilibrium model within a master-equation approach, we show the sigmoidal dependence of the detachment height on the pulling speed of the cantilever, agreeing with experimental data on a spider silk polypeptide. We also show that the slope with which the plateau forces detach is given by the cantilever force constant in both theory and experiment.

[4] Author to whom any correspondence should be addressed.

Contents

1. Introduction

In the past decade, it has become possible to directly measure the adsorption force on single polymer molecules in contact with a solid surface [1]–[15]. In these experiments, single polymer molecules are chemically attached to an atomic force microscope (AFM) tip; see figure 1. The attached polymers are then brought into contact with, and subsequently removed from, a solid surface. During this process the force $f(h)$ required to constrain the polymer at a given height h above the surface is measured. Such experiments generally show a rapid increase in the force for small heights (as the height of the end of the polymer above the surface approaches and exceeds the width of the surface potential), followed by an extended force plateau as the molecule is gradually 'peeled' off the surface, and finally a sudden drop in the force as the polymer is completely removed from the surface [1]–[15]. First theoretical analyses of equilibrium plateau forces were given in [16]–[18].

Here we readdress this problem with the aim of extracting the maximum amount of information from experiments. If a molecule is quickly removed from a surface, then nonequilibrium effects arise, which give additional information that cannot be understood in terms of thermodynamic arguments alone. To account for such nonequilibrium effects, we extend an equilibrium model within a master-equation approach, choosing for stochastic variables the height h of the end of the molecule above the surface, the end-to-end length l of the portion of the molecule on the surface and the contour length $L_c^{(h)}$ of the portion of the molecule detached from the surface. We calculate force–extension relations, height fluctuations, the dependence of the detachment height on the pulling speed and the distribution of detachment heights. We find that the dominant nonequilibrium effect is a sigmoidal dependence of the detachment height $h_{\max}$ on the pulling speed v. Our prediction of a sigmoidal dependence of the detachment height on the pulling speed has been verified by experiments on the stretching of a spider silk polypeptide.

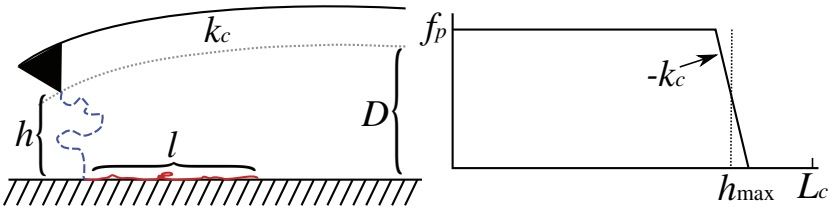

Figure 1. (Left) Schematic of pulling experiments that result in plateau forces. k_c is the force constant of the cantilever, D is the distance from the cantilever base to the substrate (corrected for the finite width of the cantilever tip), h is the height of the cantilever tip above the substrate and l is the extension of the portion of the molecule on the surface. The contour lengths $L_c^{(h)}$ and $L_c^{(s)}$ of the segments detached from and in contact with the surface are denoted by blue (dashed) and red (solid) curves, respectively. (Right) Schematic of the resulting force–extension curve indicating the plateau force f_p, the detachment height $h_{\max}$ and the contour length of the polymer L_c.

The remainder of the manuscript is organized as follows. We first present a simple derivation demonstrating that the slope of the force–extension relation following a detachment event is given by the cantilever spring constant; see figure 1. We next present equilibrium and nonequilibrium models within a single theoretical framework. Following the exposition of the theory, we present explicit numerical results for realistic parameter values. These numerical results are followed by detailed experimental results on a silk polypeptide attached to a surface, which we discuss within, and use to test, the theoretical arguments presented here. Finally, the manuscript concludes with an assessment of what has been achieved, and a discussion of future directions.

2. Mechanics: detachment slope

Here we analyse stretching with an AFM in which the cantilever base is moved away from the surface with a time dependence $D(t)$, e.g. at constant velocity v. The force on the molecule is then given by

$$f(t) = k_c(D(t) - h(t)), \tag{1}$$

where k_c is the cantilever stiffness and $h(t)$ is the position of the cantilever tip above the surface, and thus the height of the polymer detached from the surface; see figure 1. The change in force over a time interval Δt during detachment is then

$$\Delta f = k_c(\Delta D - \Delta h), \tag{2}$$

where $\Delta D = D(t + \Delta t) - D(t)$ and $\Delta h = h(t + \Delta t) - h(t)$. If detachment occurs quickly on the timescale of the changes in D (i.e. for small velocities), we can take $D(t + \Delta t) \approx D(t)$ and we obtain

$$\frac{\Delta f}{\Delta h} \approx -k_c. \tag{3}$$

In the detachment process the force drops from its plateau value to zero, i.e. $\Delta f = f_p$. Thus, only in a measurement with an infinitely stiff cantilever will the plateau force drop to zero abruptly (a discontinuity in the force–extension relation). For softer cantilevers, for which fluctuations

become substantial, plateau forces decrease linearly to zero with a slope given by the cantilever stiffness.

Note that equation (3) is valid for all force-spectroscopy experiments showing abrupt changes in force Δf. Abrupt in this context means on a timescale Δt with $k_c v \Delta t \ll \Delta f$. The velocity v does not necessarily need to be constant, as long as $|\mathrm{d}v/\mathrm{d}t|\Delta t \ll v$. Examples include the presently studied experiments showing plateau forces and also experiments on the forced unfolding of multidomain proteins, RNA hairpins and other systems [19]. Note further that the time Δt is experimentally measurable via the number of data points captured during the event in question; for the present experiments, we find that Δt is faster than or equal to data acquisition times (microseconds). Alternatively, if a given process does not obey equation (3), then this can be taken as proof that it occurs on a timescale Δt on the order of or longer than $\Delta f/(k_c v)$.

3. Thermodynamics: detachment height

As a polymer is stretched above a surface, it must eventually detach from the substrate or rupture. The polymers presently under consideration are noncovalently bonded to their substrates and thus typically detach from the surface before rupture. We define the detachment height $h_{\max}$ as the height h when the probability of the polymer being in at least partial contact with the surface drops to 50%. Clearly $h_{\max} \leqslant L_c$ for polymers of contour length L_c.

Away from equilibrium it is possible that $h_{\max}(v)$ depends on the pulling speed v. We start by considering experiments performed at such slow pulling speeds that the coupled cantilever–molecule system remains in equilibrium. The Helmholtz free energy $F(T, h, L_c)$ of the molecule can be written in terms of the temperature T, the height to which one end of the molecule is extended above the surface h and the contour length of the polymer L_c. In equilibrium the average force is $f = (\partial F/\partial h)|_{T,L_c}$, so the fact that the pulling force $f = f_p$ is constant implies that the Helmholtz free energy of the molecule is linear in the height h:

$$F(T, h, L_c) = F^{(2)}(T, L_c) + f_p h, \tag{4}$$

where $F^{(2)}$ is a function of temperature and contour length only. The detachment height $h_{eq} = h_{\max}(v = 0)$ is then given by the condition that the free energy F crosses that of the free molecule.

4. Equilibrium theory

A polymer molecule attached to a surface experiences an attractive potential arising from bonds with the surface along its backbone. This situation has been modelled as the confinement of a molecule in an external potential [18, 20]. Here we develop an approach that yields an analytical result for the equilibrium statistical mechanics by working in the Helmholtz ensemble, where one end of the molecule is fixed at a distance h above the surface. Thus part of the molecule is stretched to an extent dictated by the surface bond strength: the stronger the bond, the more the molecule outside the surface is stretched.

Under such conditions a portion of the molecule with contour length $L_c^{(h)} \leqslant L_c$ will be detached from the wall; the remaining segment with contour length $L_c^{(s)} = L_c - L_c^{(h)}$ will remain in the confining potential, gaining an extra energy $V_0 L_c^{(s)}/L_c$; see figure 1. Here V_0/L_c is the average binding energy per unit length. If the molecule remains in at least partial contact with

the surface ($L_c^{(s)} > 0$), then its partition function is

$$Z_m(L_c, h) = \frac{1}{\lambda_{th}} \int_0^{L_c} Z_h(L_c^{(h)}, h) Z_s(L_c^{(s)})\, dL_c^{(h)}, \tag{5}$$

where λ_{th} is the thermal wavelength. For brevity, we omit the explicit dependence on the temperature T from our notation. Here $Z_h(L_c^{(h)}, h)$ is the partition function of the portion of the chain outside the confining surface potential extended to an end-to-end length h above the surface. Similarly,

$$Z_s(L_c^{(s)}) = \frac{1}{\lambda_{th}} \int_0^{L_c^{(s)}} Z_s(L_c^{(s)}, l)\, dl \tag{6}$$

is the partition function of the portion of the chain in contact with the solid surface, accounting for the fact that it is free to attain any orientation and end-to-end length l. In practice, we find that the partition function $Z_s(L_c^{(s)})$ is dominated by the energy of the confining potential, $V_0 L_c^{(s)}/L_c$, which motivates the approximation

$$Z_s(L_c^{(s)}) \approx \frac{1}{\lambda_{th}} \int_0^{L_c^{(s)}} Z_h(L_c^{(s)}, l) \exp\left(\beta V_0 \frac{L_c^{(s)}}{L_c}\right) dl. \tag{7}$$

Thus far we have worked in the Helmholtz ensemble for an isolated molecule, with one end of the molecule constrained to a height h above the surface. This choice of ensembles corresponds to the limit of a stiff cantilever with respect to the molecule being stretched [21]. In actual AFM experiments, the molecule is coupled to a cantilever with finite stiffness k_c; to account for this, we must compute the partition function of the coupled cantilever–molecule system:

$$Z_{c-m}(L_c; D) = \frac{1}{\lambda_{th}} \int_0^{L_c} Z_m(L_c, h) Z_c(D - h)\, dh, \tag{8}$$

where D is the distance of the cantilever base from the substrate and

$$Z_c(D - h) = \exp\left[-\frac{\beta k_c}{2}(D - h)^2\right] \tag{9}$$

is the partition function of the cantilever.

The partition functions (5) and (8) assume that the polymer is in at least partial contact with both the AFM cantilever and the surface; this is the so-called 'bridged' or partially adsorbed state. It is of course also possible for the polymer to be completely removed from the surface. The complete partition function accounting for these two states is

$$Z_{tot}(L_c; D) = Z_{c-m}(L_c; D) + Z_f. \tag{10}$$

Here the partition function for the completely desorbed chain is given by

$$Z_f = Z_{c-m}(L_c; 0)/[\exp(\beta F_0) - 1], \tag{11}$$

where F_0 is the Helmholtz free energy required to remove the polymer from the surface. Given the partition function Z_{tot}, all quantities including force–extension curves and fluctuations can be computed as in past studies [21, 22].

Note that the free energy of adsorption F_0 differs from the binding energy V_0 due to the configurational entropy, $F_0 = V_0 - T\Delta S$. The entropy difference ΔS accounts for the fact that loops may exist in the segment of the polymer suspended between the cantilever and the substrate. However, in the calculations presented here, we find that the free energy change is due almost entirely to the confining potential, i.e. the binding energy V_0 is large compared to the change in entropy $T\Delta S$.

5. Nonequilibrium theory

Four different nonequilibrium effects can manifest themselves in pulling a molecule off a surface: (i) to change the desorbed contour length $L_c^{(h)}$, a bond with the surface has to be broken; (ii) to completely remove the molecule from the surface, several bonds have to be broken; (iii) for a new value of $L_c^{(h)}$, the end-to-end length h of the portion of the molecule not in touch with the surface has to adjust; and similarly (iv) the end-to-end length l of the portion of the molecule remaining on the surface with contour length $L_c^{(s)} = L_c - L_c^{(h)}$ must adjust. Processes (i) and (ii) are bond breaking, (iii) is internal relaxation with hydrodynamic damping the dominant effect in solution and (iv) is dominated by friction with the surface. Which of these processes are important in practice depends on the particular system under study. Nevertheless, all four phenomena can be adequately described by Markov processes.

To account for nonequilibrium effects, we treat each of $L_c^{(h)}$, h and l as stochastic variables. The function $P(L_c^{(h)}, h, l; t)$ then gives the probability that these stochastic variables attain certain values at time t; this depends implicitly on the cantilever position $D(t)$, which is itself an externally specified function of time, e.g. for constant velocity, $D = vt$. Its equilibrium form is given in terms of the partition functions as

$$P_{\mathrm{eq}}(L_c^{(h)}, h, l; D) = \frac{Z(L_c^{(h)}, h, l; D)}{Z_{\mathrm{tot}}(L_c; D)}, \tag{12}$$

where

$$Z(L_c^{(h)}, h, l; D) = Z_h(h, L_c^{(h)}) Z_s(l, L_c^{(s)}) Z_c(D-h) + \lambda_{\mathrm{th}} \delta(L_c^{(h)} - L_c) Z_f, \tag{13}$$

where the condition $L_c^{(h)} = L_c$ describes the state where the polymer is completely free, i.e. removed from the surface.

Under nonequilibrium conditions the probability distribution of a Markov process satisfies a master equation:

$$\frac{\mathrm{d}}{\mathrm{d}t} P(L_c^{(h)}, h, l; t) = \int \left[W(L_c^{(h)}, h, l; L_c^{(h)\prime}, h', l') P(L_c^{(h)\prime}, h', l'; t) - W(L_c^{(h)\prime}, h', l'; L_c^{(h)}, h, l) P(L_c^{(h)}, h, l; t) \right] \mathrm{d}L_c^{(h)\prime} \mathrm{d}h' \mathrm{d}l'. \tag{14}$$

Here $W(L_c^{(h)'}, h', l'; L_c^{(h)}, h, l)$ is the probability per unit length per unit time that there will be a transition from the state $(L_c^{(h)}, h, l)$ to the state $(L_c^{(h)'}, h', l')$. The transition probabilities must satisfy detailed balance, imposing the constraint

$$W(L_c^{(h)}, h, l; L_c^{(h)\prime}, h', l') P_{\mathrm{eq}}(L_c^{(h)\prime}, h', l'; D) \tag{15}$$

$$= W(L_c^{(h)\prime}, h', l'; L_c^{(h)}, h, l) P_{\mathrm{eq}}(L_c^{(h)}, h, l; D). \tag{16}$$

To specify the transition probabilities, we argue that the duration of individual transitions is fast on the timescale of the mesoscopic time evolution. Thus at any given time only one such transition will occur, i.e. they occur independently, and add up in the transition probabilities:

$$W(L_c^{(h)}, h, l; L_c^{(h)\prime}, h', l') = W_{\mathrm{bb}}(L_c^{(h)\prime}, L_c^{(h)}) \delta(h' - h) \delta(l' - l) + W_{\mathrm{str}}(h', h) \delta(L_c^{(h)\prime} - L_c^{(h)}) \delta(l' - l) + W_{\mathrm{fric}}(l', l) \delta(L_c^{(h)\prime} - L_c^{(h)}) \delta(h' - h). \tag{17}$$

The rate W_{bb} accounts for bond breaking, W_{str} describes the stretching of the desorbed portion of the chain (including hydrodynamic damping) and W_{fric} describes the stretching the portion of the chain in contact with the surface (including friction with the substrate).

In most experimental situations, the extension of the chain occurs on timescales fast compared to the adsorption/desorption timescales. We can thus specify the *extension* of the molecule to occur in equilibrium. The consequences of friction with the substrate have been investigated elsewhere [23]; here we focus on situations where breaking bonds with the surface is the dominant process, which is always the case for weakly bonded or physisorbed (noncovalently bonded) polymers. In this approximation, the time-dependent contour length $L_c^{(h)}(t)$ is treated as quasi-static on the timescales of the changes in the extensions h and l. Mathematically, this involves contractions over l and h,

$$Z(L_c^{(h)}; D) = \frac{1}{\lambda_{th}^2} \int_0^{L_c^{(h)}} \int_0^{L_c^{(s)}} Z(L_c^{(h)}, h, l; D)\, dh\, dl, \tag{18}$$

and defines the equilibrium probability $P_{eq}(L_c^{(h)}; D)$ that a contour length $L_c^{(h)}$ is outside of the surface potential when the end of the cantilever is fixed at a distance D from the substrate:

$$P_{eq}(L_c^{(h)}; D) = \frac{Z(L_c^{(h)}; D)}{Z(D)}, \tag{19}$$

where

$$Z(D) = \frac{1}{\lambda_{th}} \int_0^{L_c} Z(L_c^{(h)}; D)\, dL_c^{(h)}. \tag{20}$$

The probability $P(L_c^{(h)}; t)$ may then be subjected to a master equation:

$$\frac{d}{dt} P(L_c^{(h)}; t) = \int dL_c^{(h')} \left[W_{bb}(L_c^{(h)}, L_c^{(h')}) P(L_c^{(h')}; t) - W_{bb}(L_c^{(h')}, L_c^{(h)}) P(L_c^{(h)}; t) \right]. \tag{21}$$

6. Two-state detachment

We now consider the bond breaking rates W_{bb}. Monomers are sequentially removed from the surface and there are energetic barriers to desorbing each monomer. However, if $h_{max} \neq L_c$ then multiple monomers must be removed within a short time period during detachment. One expects the removal of individual monomers to be a fast process compared to the removal of many monomers; this motivates an approximation where individual monomers are quasi-statically 'peeled' off the surface, until eventually all monomers remaining on the surface are abruptly removed in a two-state process; see figure 2.

To formulate the resulting two-state model we define P_b, the probability that the polymer is in at least partial contact with the surface (bridged), and $P_f = 1 - P_b$, the probability that the polymer has been completely removed from the surface (free). In equilibrium these probabilities depend only on the cantilever position D, and we have

$$P_b^{(eq)}(D) = \frac{Z_{c-m}(L_c; D)}{Z_{c-m}(L_c; D) + Z_f}. \tag{22}$$

Out of equilibrium the probabilities $P_b(t)$ and $P_f(t) = 1 - P_b(t)$ obey a master equation:

$$\frac{dP_b}{dt} = W_{bf}(D) P_f - W_{fb}(D) P_b. \tag{23}$$

Here the transition rate W_{fb} describes the detachment of several monomers from the substrate at the end of the desorption process, i.e. the transition rate from the state depicted in figure 2(d) to that of figure 2(e). Conversely, W_{bf} refers to the reverse process (reattachment), which may

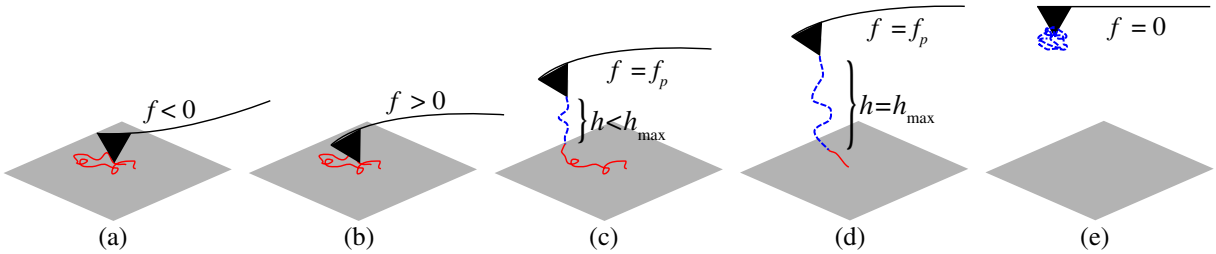

Figure 2. Schematic illustrating five stages in the forced desorption of a polymer from a surface according to our analysis. (a) The AFM tip is pushed against the substrate, with the aim of adsorbing a single molecule. (b) The direction of applied force is reversed; because of the surface potential, the polymer and cantilever will remain 'stuck' to the surface for forces below the plateau force f_p. (c) The cantilever is moved away from the surface at a constant velocity v, sequentially removing monomers from the surface potential. (d) The polymer is extended to a critical height h_{max}. (e) Immediately following time point (d), the force drops abruptly to zero, and all monomers remaining within the confining potential are removed from the surface. The polymer need not be extended to its contour length for this to occur. Transitions from the bridged state (d) to the free state (e) occur with rate W_{fb}; transitions from the free state (e) to the bridged state (d) occur with rate W_{bf}.

or may not be an important process, depending on the pulling speeds and the particular system being investigated.

Equation (23) follows from equation (21), given the assumption that adsorption and desorption of individual monomers are fast on the timescale of desorption of the whole chain. For fixed cantilever position D, the master equation (equation (23)) is solvable analytically, and we find

$$P_b(t) = \frac{W_{bf}}{W_{bf}+W_{fb}} + \left(P_b(0) - \frac{W_{bf}}{W_{bf}+W_{fb}}\right)\exp[-(W_{bf}+W_{fb})t]. \tag{24}$$

The time evolution $P_b(t)$ for arbitrary cantilever motion $D(t)$ can be obtained numerically by repeatedly applying equation (24) over short intervals (short compared to the rate of change of the cantilever position $D(t)$).

To complete the model we require explicit forms for the rates W_{bf} and W_{fb}. Such rates must satisfy detailed balance:

$$W_{bf}(D)Z_f = W_{fb}(D)Z_{c-m}(L_c; D), \tag{25}$$

and can thus be written in the form

$$\begin{aligned} W_{bf}(D) &= \omega_0 \left(\frac{Z_{c-m}(L_c; D)}{Z_f}\right)^{1-c}, \\ W_{fb}(D) &= \omega_0 \left(\frac{Z_{c-m}(L_c; D)}{Z_f}\right)^{-c}, \end{aligned} \tag{26}$$

for some $c \in [0, 1]$. The value of the constant c determines the degree to which tension on the molecule increases the desorption rate; we comment further on the parameter c in the next

section. We have taken the simplest possible choice for these rates, namely that the rates are linear in an attempt frequency ν, and depend exponentially on a barrier height Q. These two effects can be combined into a single effective transition frequency $\omega_0 = \nu \exp(-\beta Q)$.

Note that we have constructed the rates W_{bf} and W_{fb} based on the fact that they must obey detailed balance. An alternative approach would be to postulate the forward rate W_{fb} based on physical grounds and neglect the reverse transition rates W_{bf}. This is done, for example, in the Bell model (see appendix A). The latter, frequently used to describe bond breaking, is of limited use for the present problem because it only accounts for bond breaking (our rate W_{fb}) but not for reattachment (our rate W_{bf}), so that detailed balance is not satisfied. Recall that reattachment refers to the transition from the free state depicted in figure 2(e) to the bridged state depicted in figure 2(d). For a given experimental situation (e.g. high pulling speeds), reattachment may be a very unlikely process. However, reattachment is crucial for slow pulling speeds where one stays close to equilibrium. In general, both bond breaking and reattachment can occur, and the master equation accounts for both these processes.

The polymer is assumed to maintain a local equilibrium in each of its two possible states: while in contact with the surface, the height h of the polymer adjusts quickly on the timescales of the cantilever position $D(t)$; the probability distribution function of the height in this state is that of equilibrium. Similarly, when the polymer is out of contact with the surface and the cantilever relaxes ($f = 0$), it is assumed that the polymer's end-to-end distance maintains local equilibrium. The force and height in this approximation are then computed as in appendix B.

7. Theoretical results

We now present explicit numerical results for the situation where removing a polymer from a surface is well modelled as a two-state Markov process. In this model a polymer is assumed to maintain local equilibrium in each of the two states, namely bridged between the AFM cantilever and the surface, or completely detached from the surface.

First, let us consider the results of this model in the equilibrium limit (low pulling speeds). The force–extension curve and the corresponding fluctuations are shown in figures 3(a) and (b) (solid curves). As expected, the model predicts a plateau force up to a given height h_{max}, where the force drops abruptly to zero. Interestingly, for the chosen parameter values (given in the figure caption), we find $h_{\mathrm{max}} \approx 0.5 L_{\mathrm{c}}$, i.e. the detachment height h_{max} is significantly smaller than the contour length L_{c} under equilibrium conditions.

Next, we find that this model predicts an enhancement of the detachment height h_{max} with velocity v (an increase in the maximum height before the polymer detaches from the surface); see figure 3(a). For values of c close to zero, we find that this enhancement is significant and can cause the detachment height to asymptotically approach the contour length of the polymer. Considering the limit of high pulling speed reveals an important insight: the force on an adsorbed polymer would necessarily diverge (or fracture the polymer) before the detachment height reached the contour length of the polymer. This follows simply from the fact that any force–extension curve diverges for a polymer in the standard pulling geometry (attached firmly to the surface). The beginnings of this enhanced force are visible in the highest velocity (dash-dot-dot curve) of figure 3(a). Thus, experiments involving the removal of polymers from surfaces will necessarily see desorption of the polymer chain at heights less than the contour length of the polymer (stretching of individual covalent bonds and covalent-bond angles can be neglected at forces below 100 pN [24]).

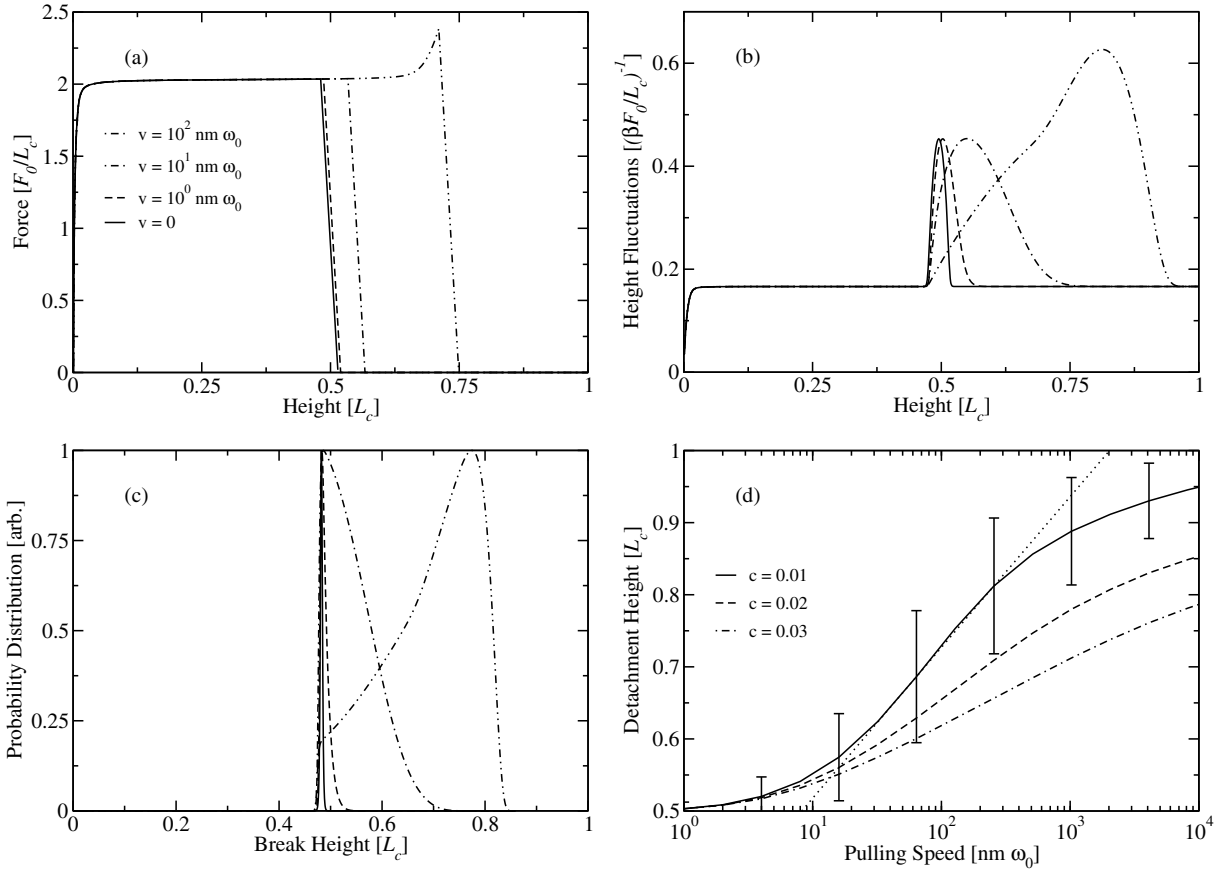

Figure 3. Nonequilibrium force–extension curves calculated in a two-state model of desorption. (a) Force–extension curves, showing an enhancement of the detachment height with pulling speed. (b) Height fluctuations, revealing a broadening and eventual enhancement of the fluctuations with pulling speed, centred around the detachment height $h_{\max}$. (c) Probability distribution of detachment heights. All probability densities have been normalized to have equal maxima for plotting purposes. Common parameters for panels (a)–(c): $v = 10^0, 10^1, 10^2$ nm ω_0 for dashed, dash-dot, dash-dot-dot curves, respectively. All curves have detailed balance exponents $c = 0.01$. Solid curves are calculated in equilibrium. (d) Dependence of detachment height on pulling speed. Error bars are computed as the standard deviation of the distribution as in panel (c); for clarity of the plot, these are presented only for one curve ($c = 0.01$), but values are representative of all three curves. The logarithmic dependence for intermediate velocities is shown as a dotted line. Parameters: solid, dashed and dash-dot curves have detailed balance exponents $c = 0.01$, 0.02 and 0.03, respectively. Parameters common to all panels are $T = 300$ K, $L_c = 100$ nm, $L_p = 0.4$ nm, $k_c = 10$ pN nm^{-1} and $F_0/L_c = 100$ meV nm^{-1}.

Due to thermal fluctuations of the coupled cantilever–molecule system, the height h of the cantilever tip above the substrate undergoes height fluctuations δh; see figure 3(b). We find that the dominant nonequilibrium effect is a broadening and enhancement of the height fluctuations around the detachment height. The origins of this nonequilibrium effect are as follows. As the

height h is increased, the probability P_b that the molecule remain in contact with the surface decreases. In equilibrium, the probability P_b drops sharply at the detachment height h_{max} (data not shown). Out of equilibrium the molecule takes longer on average to detach from the surface. Due to this delay in detachment, the polymer becomes stretched to a height $h > h_{eq}$, where it is unstable. In this context, unstable implies that, for these heights h, if the system were allowed to equilibrate then the polymer would detach from the surface. It is this region of instability that leads to the large height fluctuations shown in figure 3(b).

Thus far we have defined h_{max} as the height h when the probability of the polymer being in at least partial contact with the surface drops to 50%. However, detachment heights are stochastic and are distributed around this value. Distributions of the detachment heights for various pulling speeds are presented in figure 3(c). Again, we find that the dominant nonequilibrium effect is to broaden the distribution of detachment heights.

Next, in figure 3(d) we present the dependence of detachment height on pulling speed. For intermediate velocities this dependence appears logarithmic (dotted curve), which is what is typically reported experimentally and predicted by Bell-like models (see appendix A). On the other hand, in the limit of low pulling speed the detachment height of the polymer must converge to its equilibrium value. Similarly, in the limit of high pulling speed the detachment height approaches the contour length of the polymer. Thus, the dependence of detachment height on pulling speed necessarily varies sigmoidally from its equilibrium value at zero pulling speed to the contour length of the polymer at infinite pulling speed. At the highest pulling speeds the detachment height approaches the contour length; see figure 3(d).

Our model predicts that applied force increases the desorption rate W_{fb} and decreases the adsorption rate W_{bf}. This is implied by detailed balance, equation (25). The relative magnitude of the effect of force on adsorption versus desorption is captured by an exponent c. For $c = 0$ the desorption rate is independent of the applied force and the adsorption rate depends most strongly on the force. Similarly, for $c = 1$ the adsorption rate is force independent. By controlling the desorption time, the exponent c determines the degree to which the detachment height $h_{max}(v)$ depends on the velocity v; see figure 3(d). In practice, we find that the behaviour of the model most closely resembles that of experiment for values of $c \approx 0.01$. For larger values of $c \approx 1$ the polymer rapidly detaches from the substrate for heights $h > h_{eq}$, and we find that the detachment height $h_{max}(v) \approx 0.5L_c$ for all pulling speeds investigated (data not shown). An analysis similar to the one presented in appendix A shows that, at least approximately, the slope of h_{max} versus $\log(v/v_0)$ is given by $1/(\beta f_p L_c c)$ for intermediate velocities v, and v_0 any reference velocity. Thus, the value of $c \approx 0.01$ found here should be compared to $1/(\beta f_p L_c)$, a number on the order of 10^{-3} for the parameters under study.

Finally, we note that the plateau force f_p in our model is independent of the pulling speed; see figure 3(a). This fact follows from the assumption that the polymer maintains local equilibrium while bridged between the AFM cantilever and the surface. In order to show how the plateau force depends on the *equilibrium* model parameters, we present in figure 4 force–extension curves for our model in the limit of low pulling speeds, for various values of the parameters L_c, L_p, k_c and F_0. We find that the plateau force f_p is independent of both the contour length L_c and the cantilever spring constant k_c, as long as the free energy of adsorption per unit length F_0/L_c is constant; see figures 4(a) and (b). Meanwhile, as either persistence length L_p or binding energy F_0 is increased, entropic effects become negligible and the plateau force approaches F_0/L_c; see figures 4(c) and (d).

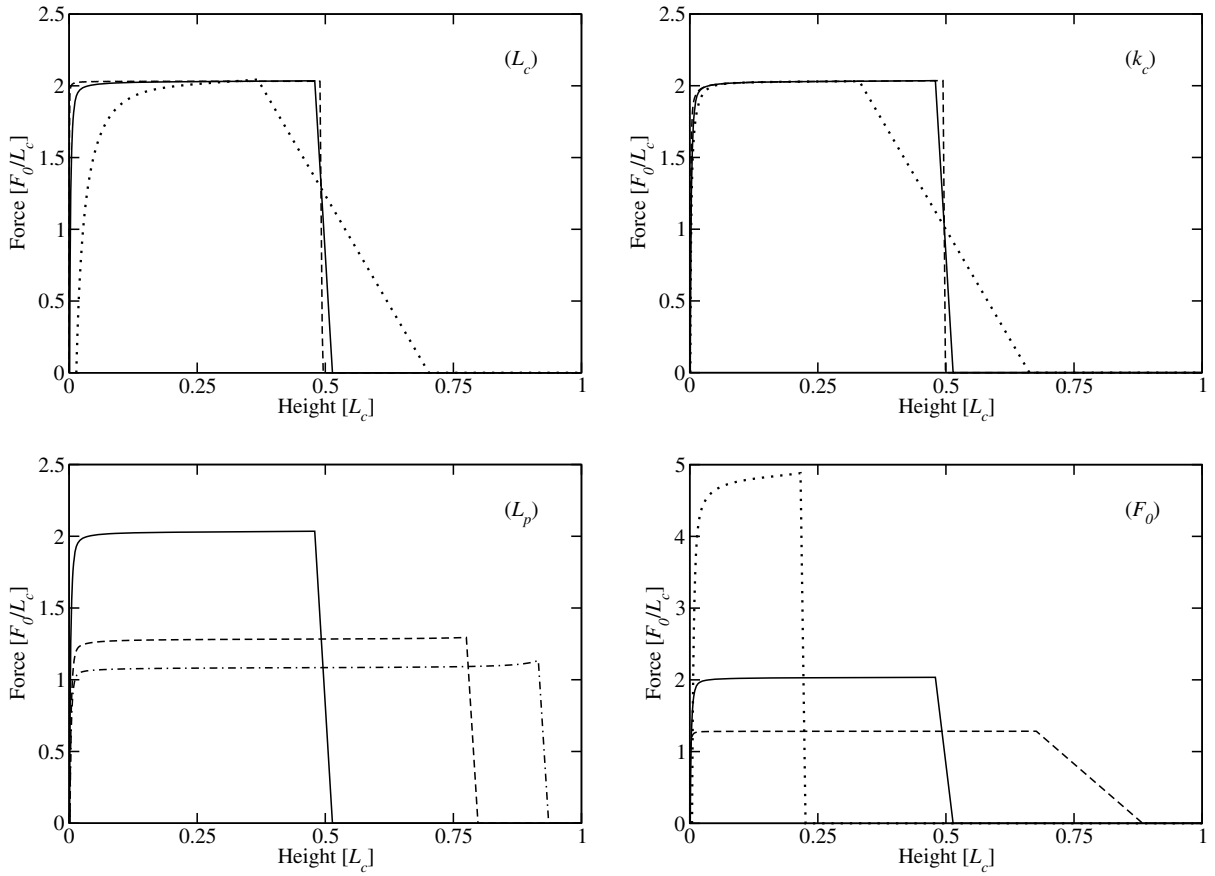

Figure 4. Equilibrium force–extension curves for polymer adsorption with varying parameter values. The solid curve is common to each panel and has parameters $L_c = 100\,\text{nm}$, $L_p = 0.4\,\text{nm}$, $k_c = 10\,\text{pN nm}^{-1}$ and $F_0/L_c = 100\,\text{meV nm}^{-1}$. Forces are plotted in the natural units of the adsorption strength, F_0/L_c, and lengths are plotted in units of L_c. Panels (L_c), (k_c), (L_p) and (F_0) show the variations of the master force–extension curve with each of these parameters, respectively, with all other parameters fixed as in the solid curve above. The temperature is fixed at $T = 300\,\text{K}$ for all curves. Parameters for individual panels are as follows. (L_c): dotted, solid, dashed curves have $L_c = 10$, 100, 1000 nm, respectively. (k_c): dotted, solid, dashed curves have $k_c = 1$, 10, 100 pN nm^{-1}, respectively. (L_p): solid, dashed, dash-dot curves have $L_p = 0.4$, 4, 40 nm, respectively. (F_0): dotted, solid, dashed curves have $F_0/L_c = 10$, 100, 1000 meV nm^{-1}, respectively.

8. Experimental results

In practice, the polymer of interest is covalently bound to the apex of an AFM cantilever tip using a flexible linker molecule, such as poly(ethylene glycol) (PEG) (4). Hence experimentally we are dealing with a composite chain. The contour length L_c and the persistence length L_p used in the theoretical analysis refer to the sum of the contour lengths of the polymer and linker molecule, and an effective persistence length of the polymer chain plus linker, respectively.

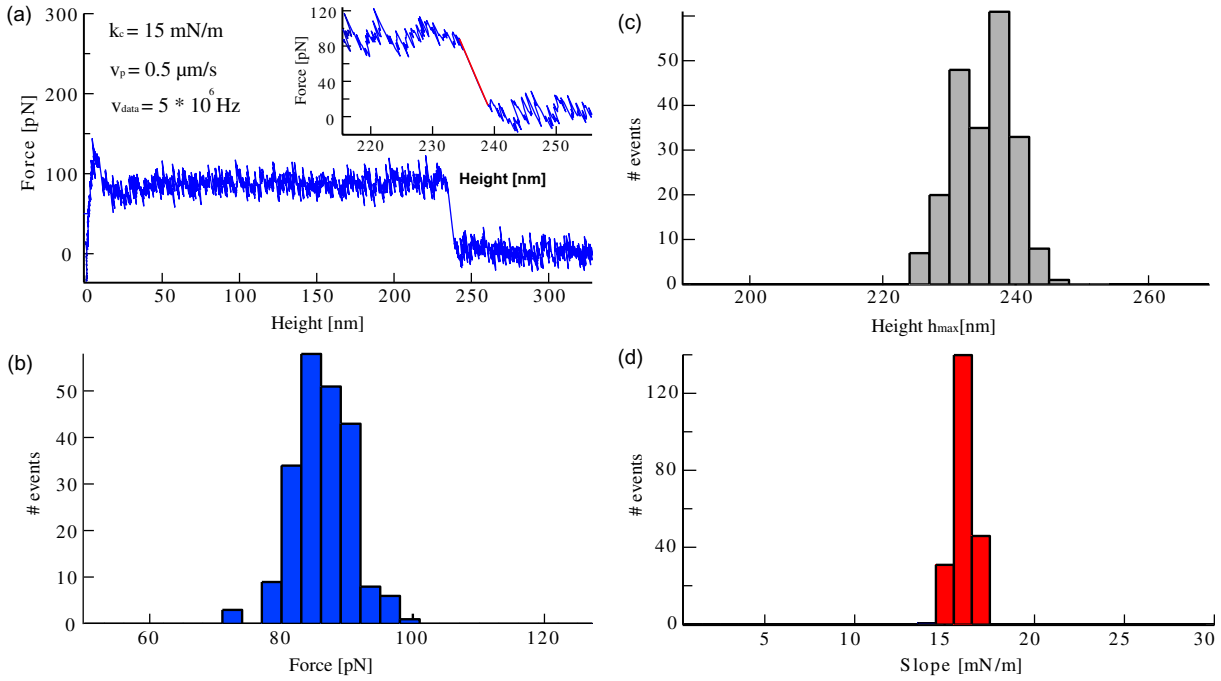

Figure 5. Single-molecule force spectroscopy using AFM. (a) A typical force–separation curve of eADF4 from H-diamond in K_2HPO_4 solution (500 mM) at room temperature. The retract velocity is 1 μm s^{-1}. The inset highlights the detachment slope of the curve. (b) Distribution of desorption forces obtained with one and the same molecule, (c) corresponding detachment heights h_{max} and (d) detachment slopes. The histograms comprise 220 desorption events.

As an example, we present a set of experimental data obtained with an engineered spider silk protein eADF4 (C16) whose amino acid sequence was adapted from the natural sequence of the dragline silk fibroin of *Araneus diadematus* ADF4 (see appendix C). The engineering approach allowed the multimerization of single repeats (C-motif), resulting in a molecular weight (MW) of 48 kDa for C16. Based on the amino acid sequence, eADF4 exhibits a well-defined contour length of 210 nm. Three different PEG linker molecules of contour lengths 1, 16 and 49 nm were used to attach eADF4 to the AFM tip. The substrate surface in this study was hydrogenated diamond (H-diamond). The aim of the experiments is to investigate the pulling velocity dependence of the plateau height and length.

Prior to each desorption experiment, the cantilever spring constant k_c was determined with a common uncertainty of 12% (see appendix C). A typical set of data comprises several hundred force–separation curves as the example depicted in figure 5(a), which provide three basic parameters: the average plateau force f_p (figure 5(b)), the average plateau length h_{max} (figure 5(c)) and the average value of the detachment slope (figures 5(a) and (d)).

As expected, the detachment slope is finite and equal to $-k_c$ (figures 5(a) and (d)). This prediction of our thermodynamics analysis was tested by plotting the average detachment slope as a function of the estimated spring constant k_c for 45 different experiments and cantilevers with bound eADF4, respectively (figure 6). The detachment slope reflects the cantilever spring constant one to one independently of the length of linker used, of the pulling velocity (500 or

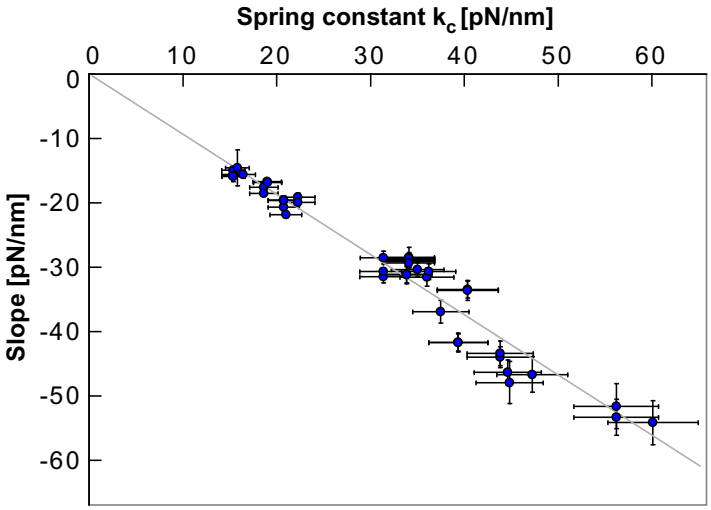

Figure 6. Detachment slope as a function of the cantilever spring constant k_c. The graph depicts 45 different desorption experiments of eADF4 with varying PEG linker length, salt concentration and temperature. The slope equals $-k_c$ regardless of the experimental conditions. Error bars are defined as three times the standard error.

1000 nm s^{-1}), of the ionic strength of the electrolyte solution (ranging from 20 to 500 mM) and of the temperature (25–47 °C).

Finally, we present in figures 7 and 8 the dependence of the detachment height h_{max} on the pulling velocity, with the aim of testing the theoretical predictions of the preceding sections. Indeed, only for the highest pulling speeds (2500 and 4020 nm s^{-1}) does the experimental detachment height h_{max} approach the contour length L_c (indicated as a blue line in figure 7). Furthermore, plotting the average value of the detachment height as a function of pulling speed (figure 8), we see that for pulling speeds $v \lesssim 100$ nm s^{-1} the detachment height h_{max} appears to converge to a value of the order of 50% of the contour length of the composite PEG-spider silk chain. This suggests that equilibrium may be achieved for experiments performed with pulling speeds $v \lesssim 100$ nm s^{-1}. Note that the experimental pulling speeds were not sufficient to show the complete sigmoidal dependence of h_{max} on v as predicted in figure 3(d). However, the experimental data presented here are consistent with and point in the same direction as our theoretical analysis.

9. Conclusions

In the recent past, atomic force microscopy (AFM) experiments have been developed to accurately measure the forces necessary to desorb a single polymer chain from a surface in aqueous solution. In a large class of such desorption experiments, the observation of single plateaus of constant force is the hallmark of the forced desorption of a single polymer chain physisorbed at the substrate surface. The conditions under which such plateau forces are expected to become observable have been reviewed previously from an experimental [3] and theoretical point of view [18].

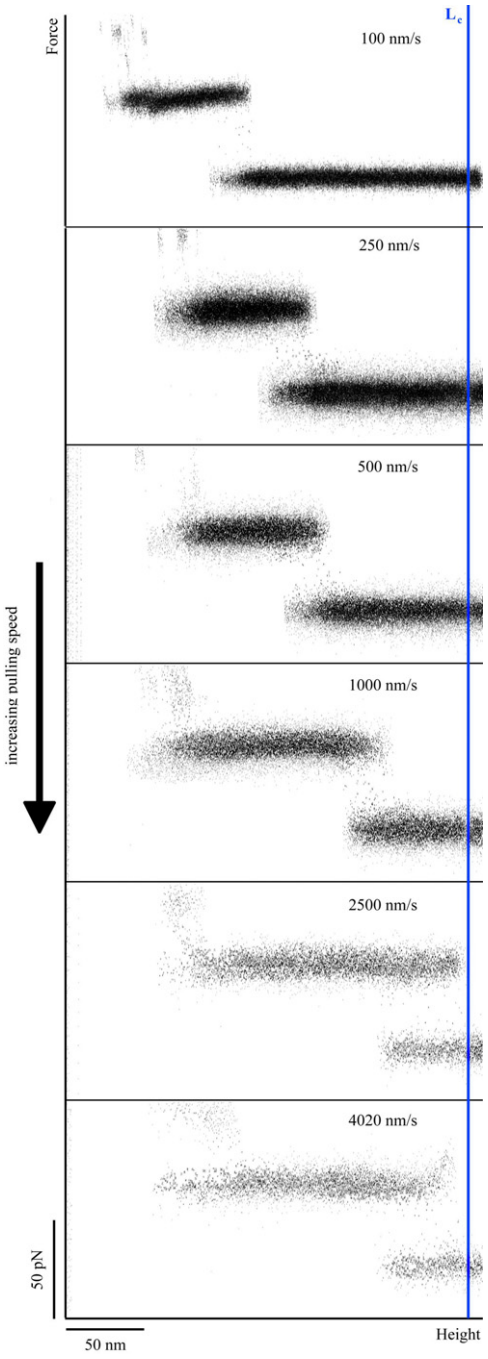

Figure 7. Dependence of detachment height on pulling velocity. For each experiment with different velocity, the superposition of 20 typical retract curves is shown. With increasing retract speed, the plateau elongates and the measured detachment height $h_{\max}$ approaches the contour length L_c of protein plus linker (height increases to the right). Here the contour length of the PEG linker was $\sim$49 nm, such that the contour length of the composite chain was $L_c \approx 259$ nm. The data acquisition rate of 5×10^6 Hz was kept constant. High-force points for small heights result from nonspecific interactions of the cantilever tip with the substrate.

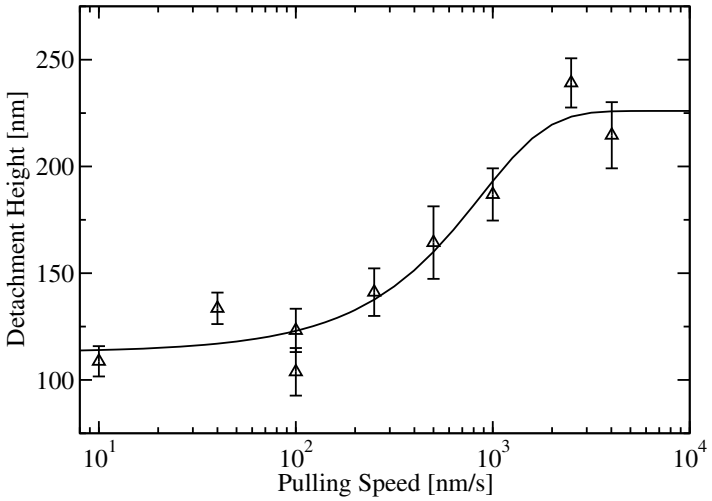

Figure 8. Detachment height h_{max} as a function of pulling velocity. Each data point represents the average value of h_{max} from approximately 200 experimental traces. Error bars are defined as in figure 6. Contour length, linker molecules and data acquisition rates are as in figure 7. The solid curve is a sigmoidal fit added as a guide to the eye.

Here we have revisited this problem with the aim of developing a consistent theoretical framework in which we can answer the question: what can be learnt from plateau forces? Firstly, we find that the slope with which the force decays to zero after the polymer has ruptured its last surface bond is given by the inverse of the cantilever force constant; see equation (3) and figure 6. Our theoretical analysis shows that this fact holds both in and out of equilibrium, as long as detachment occurs on a timescale Δt with $k_c v \Delta t \ll \Delta f$. This condition is fulfilled under all experimental conditions investigated, and this fact can thus serve as an excellent check on the quality of the experimental results.

Next, we show that physisorbed polymers, such as spider silk, are well described by a local equilibrium while in contact with a solid surface. To describe the dominant nonequilibrium effects, we invoke a two-state Markov process describing the complete detachment of the chain from the surface. In this model, the plateau force is necessarily unaffected by the pulling speed of the cantilever. However, we find that the plateau force depends on the persistence length of the polymer L_p and the free energy of adsorption F_0. Furthermore, we find both theoretically and experimentally that the detachment height $h_{max}(v)$ varies sigmoidally as a function of velocity, from its equilibrium value h_{eq} at low pulling speeds ($<100\,\mathrm{nm\,s^{-1}}$ for the investigated spider silk), approaching the contour length L_c of the polymer being stretched for high pulling speeds ($>2500\,\mathrm{nm\,s^{-1}}$ for the investigated spider silk).

In this study, we present experimental results motivated by theoretical calculations. However, we do not present a high-precision comparison between experiment and numerical results of our theoretical model. Here the logic is to elucidate the key theoretical and experimental mechanisms in a general context. However, it would be interesting for future study to make direct numerical comparisons between theory and experiment under a wide range of experimental conditions. Finally, given a nonequilibrium theoretical model and appropriately designed experiments, it should be possible to extract molecular relaxation times

from experimental data. We hope that the results presented in this study provide the necessary theoretical foundations to solve these additional problems, leading to a complete theoretical understanding of the experimental data.

Acknowledgments

This work was supported by grants from NSERC, the Office of Naval Research and the German Science Foundation (DFG, HU 997/2). DS would like to acknowledge scholarships from NSERC and DAAD. MG was supported by the Elitenetzwerk Bayern in the framework of the doctorate programme Material Science of Complex Interfaces and the Stiftung Industrieforschung.

Appendix A. Computing $h_{\max}(v)$ in the Bell model

In a typical Bell-like model, the probability that the polymer has been completely removed from the surface is written as

$$P_{\mathrm{f}}(t) = 1 - \exp\left[\int_0^t W_{\mathrm{fb}}(t')\,\mathrm{d}t'\right], \tag{A.1}$$

with an exponentially dependent desorption rate

$$W_{\mathrm{fb}} = k_0 \exp(\beta f_0 h), \tag{A.2}$$

where f_0 is an energy per unit length and we have included any reference height h_0 in the attempt frequency k_0. Imposing a linearly increasing height $h = vt$ and solving $P_{\mathrm{f}} = 1/2$ yields an analytic expression for the expected detachment height:

$$h_{\max} = \frac{1}{\beta f_0} \ln\left(\frac{\ln 2 \beta f_0}{k_0} v + 1\right). \tag{A.3}$$

The functional dependence is thus $h_{\max} \sim \ln(v/v_0 + 1)$, where $v_0 = \beta f_0 \ln 2/k_0$, i.e. $h_{\max}(v)$ in the above Bell model is logarithmic for sufficiently high velocities, and decays to zero in the limit of low pulling speed ($h_{\max}(0) = 0$).

Appendix B. Computing force–extension curves

AFM measurements do not yield ensemble averages of partially adsorbed (bridged) or completely desorbed (free) polymers. Rather, experimentalists measure the stochastic desorption of the chain from the surface, visible as a sharp drop in the force. For this reason we define the force in our two-state model as

$$f = \left.\frac{\partial F_{\mathrm{c-m}}(L_{\mathrm{c}}; D)}{\partial D}\right|_{T, L_{\mathrm{c}}} \qquad (P_{\mathrm{b}} < 0.5) \tag{B.1}$$

$$= 0 \qquad (P_{\mathrm{b}} \geqslant 0.5), \tag{B.2}$$

where $F_{c-m}(L_c; D) = -k_B T \ln Z_{c-m}(L_c; D)$. The height $h = D - f/k_c$ is subsequently defined in terms of the force f and cantilever position D.

Appendix C. Materials and methods

C.1. Hydrogenated diamond substrate

Hydrogenation of polished polycrystalline diamond surfaces (ElementSix Advancing Diamond Ltd, UK) was conducted as described elsewhere [25]. Briefly, after acidic treatment to clean the surface from possible contaminants, the samples were heated in a vacuum chamber to a temperature of 700 °C at a pressure of 5×10^{-7} mbar. The hot sample surface was exposed to hydrogen radicals generated by two 2100 °C hot tungsten filaments for 30 min at a controlled pressure of 1.5 mbar, and cooled in hydrogen atmosphere. The H-terminated diamond surfaces were hydrophobic with contact angles between 80° and 90°. The specimens were wiped clean followed by ultrasonic cleaning in acetone, 2-propanol and pure water before measurements.

C.2. Recombinant spider silk protein

We use a genetically engineered polypeptide derived from ADF4 (*Araneus diadematus fibroin*) of the garden cross spider. The protein eADF4 was recombinantly produced in *Escherichia coli* and purified as described previously [26]. Spider silk eADF4 exhibits no intrinsic structure in aqueous solution at room temperature [27].

C.3. Single-molecule force spectroscopy

The preparation of the AFM cantilever tips (MLCT-AUHW, Veeco, Germany) and attachment of single eADF4 molecules have been described earlier [28]. All experiments were performed in aqueous solution with an MFP-3D with Bioheater (Asylum Research). During indentation of the tip, the molecule is allowed to adsorb at the diamond surface for 1 s before the cantilever is retracted at constant velocity. Force–separation traces were derived from the deflection-piezopath signal [3].

The spring constant of each cantilever was determined before the measurement by integrating over the power spectral density from 75 Hz to the local minimum between the first and the second resonance peaks, and by applying the equipartition theorem [29]. The optical lever sensitivity was averaged over the first five and the last five retraction curves.

Each force value in this study was determined from a histogram built from at least 200 force–separation traces. The corresponding standard deviations were calculated according to the theory of small samples. The main uncertainty stems from cantilever calibration [30]. We therefore used one and the same cantilever to obtain all data points at different velocities. The uncertainties thus do not give the uncertainties of absolute values but rather represent the relative error of the measurements.

References

[1] Châtellier X, Senden T J, Joanny J-F and di Meglio J-M 1998 Detachment of a single polyelectrolyte chain adsorbed on a charged surface *Europhys. Lett.* **41** 303–8

[2] Senden T J, di Meglio J-M and Auroy P 1998 Anomalous adhesion in adsorbed polymer layers *Eur. Phys. J.* B **3** 211–6

[3] Hugel T and Seitz M 2001 The study of molecular interactions by AFM force spectroscopy *Macromol. Rapid Commun.* **22** 989–1016
[4] Cui S, Liu C and Zhang X 2003 Simple method to isolate single polymer chains for the direct measurement of the desorption force *Nano Lett.* **3** 245–8
[5] Friedsam C, del Campo Bécares A, Jonas U, Seitz M and Gaub H E 2004 Adsorption of polyacrylic acid on self-assembled monolayers investigated by single-molecule force spectroscopy *New. J. Phys.* **6** 9–16
[6] Kellermayer M S Z, Grama L, Karsai Á, Nagy A, Kahn A, Datki Z L and Penke B 2005 Reversible mechanical unzipping of amyloid β-fibrils *J. Biol. Chem.* **280** 8464–70
[7] Sun M, Graham J S, Hegedus B, Marga F, Zhang Y, Forgacs G and Grandbois M 2005 Multiple membrane tethers probed by atomic force microscopy *Biophys. J.* **89** 4320–9
[8] Kiss B, Karsai Á and Kellermayer M S Z 2006 Nanomechanical properties of desmin intermediate filaments *J. Struct. Biol.* **155** 327–39
[9] Karsai Á, Mártonfalvi Zs, Nagy A, Grama L, Penke B and Kellermayer M S Z 2006 Mechanical manipulation of Alzheimer's amyloid β1-42 fibrils *J. Struct. Biol.* **155** 316–26
[10] Sonnenberg L, Luo Y, Schlaad H, Seitz M, Colfen H and Gaub H E 2007 Quantitative single molecule measurements on the interaction forces of poly(l-glutamic acid) with calcite crystals *J. Am. Chem. Soc.* **129** 15364–71
[11] Yu Y, Wang F, Shi W, Wang L, Wang W and Shen J 2008 Conformations and adsorption behavior of poly(allylamine hydrochloride) studied by single molecule force spectroscopy *Chin. Sci. Bull.* **53** 22–6
[12] Horinek D, Serr A, Geisler M, Pirzer T, Slotta U, Lud S Q, Garrido J A, Scheibel T, Hugel T and Netz R R 2008 Peptide adsorption on a hydrophobic surface results from an interplay of solvation, surface and intrapeptide forces *Proc. Natl Acad. Sci. USA* **105** 2842–7
[13] Manohar S, Mantz A R, Bancroft K E, Hui C-Y, Jagota A and Vezenov D V 2008 Peeling single-stranded DNA from graphite surface to determine oligonucleotide binding energy by force spectroscopy *Nano Lett.* **8** 4365–72
[14] Weinman C J, Gunari N, Krishnan S, Dong R, Paik M Y, Sohn K E, Walker G C, Kramer E J, Fischer D A and Ober C K 2010 Protein adsorption resistance of anti-biofouling block copolymers containing amphiphilic side chains *Soft Matter* **6** 3237–43
[15] Geisler M, Netz R R and Hugel T 2010 Pulling a single polymer molecule off a substrate reveals the binding thermodynamics of cosolutes *Angew. Chem. Int. Ed.* **49** 4730–3
[16] Châtellier X and Joanny J-F 1998 Pull-off of a polyelectrolyte chain from an oppositely charged surface *Phys. Rev.* E **57** 6923–35
[17] Klushin L I, Skvortsov A M and Leermakers F A M 2002 Exactly solvable model with stable and metastable states for a polymer chain near an adsorbing surface *Phys. Rev.* E **66** 036114
[18] Hanke F, Livadaru L and Kreuzer H J 2005 Adsorption forces on a single polymer molecule in contact with a solid surface *Europhys. Lett.* **69** 242–8
[19] Staple D B, Payne S H, Reddin A L C and Kreuzer H J 2008 Model for stretching and unfolding the giant multidomain muscle protein using single-molecule force spectroscopy *Phys. Rev. Lett.* **101** 248301
[20] Hanke F and Kreuzer H J 2006 Breaking bonds in the atomic force microscope: theory and analysis *Phys. Rev.* E **74** 031909
[21] Kreuzer H J, Payne S H and Livadaru L 2001 Stretching a macromolecule in an atomic force microscope: statistical mechanical analysis *Biophys. J.* **80** 2505–14
[22] Staple D B, Hanke F and Kreuzer H J 2008 Dynamics of single-molecule force-ramp experiments: the role of fluctuations *Phys. Rev.* E **77** 021801
[23] Serr A and Netz R R 2006 Pulling adsorbed polymers from surfaces with the AFM: stick versus slip, peeling versus gliding *Europhys. Lett.* **73** 292–8
[24] Hugel T, Rief M, Seitz M, Gaub H E and Netz R R 2005 Highly stretched single polymers: atomic-force-microscope experiments versus *ab-initio* theory *Phys. Rev. Lett.* **94** 048301

[25] Härtl A, Garrido J A, Nowy S, Zimmermann R, Werner C, Horinek D, Netz R R and Stutzmann M 2007 The ion sensitivity of surface conductive single crystalline diamond *J. Am. Chem. Soc.* **129** 1287–92
[26] Rammensee S, Slotta U, Scheibel T and Bausch A R 2008 Assembly mechanism of recombinant spider silk proteins *Proc. Natl Acad. Sci. USA* **105** 6590–5
[27] Exler J H, Hümmerich D and Scheibel T 2007 The amphiphilic properties of spider silks are important for spinning *Angew. Chem. Int. Ed.* **46** 3559–62
[28] Geisler M, Pirzer T, Ackerschott C, Lud S, Garrido J, Scheibel T and Hugel T 2008 Hydrophobic and Hofmeister effects on the adhesion of spider silk proteins onto solid substrates: an AFM-based single-molecule study *Langmuir* **24** 1350–5
[29] Butt H-J and Jaschke M 1995 Calculation of thermal noise in atomic force microscopy *Nanotechnology* **6** 1–7
[30] Pirzer T, Geisler M, Scheibel T and Hugel T 2009 Single molecule force measurements delineate salt, pH and surface effects on biopolymer adhesion *Phys. Biol.* **6** 025004